Testbed-based Receiver Optimization for SISO Molecular Communication Channels

Pit Hofmann*, Jorge Torres Gómez‡, Falko Dressler‡, and Frank H.P. Fitzek*†
*Deutsche Telekom Chair of Communication Networks, Technische Universität Dresden, Germany
†Centre for Tactile Internet with Human-in-the-Loop (CeTI), Dresden, Germany
‡School for Electrical Engineering and Computer Science, TU Berlin, Berlin, Germany
{pit.hofmann, frank.fitzek}@tu-dresden.de, {torres-gomez, dressler}@ccs-labs.org

***Abstract*—When conceiving molecular communication (MC) systems, it is of utmost importance to determine the threshold value for decoding bits and producing the smaller bit error rate (BER). At this optimum, the BER has the smallest value, and errors in the reception can be minimized, thereby improving the minimal throughput of molecular means. Despite its importance, prior research still presents little applicability and insights obtaining the optimal threshold for real testbeds. Filling this gap, in this paper, we feature a low-complex algorithm for the optimal threshold in single-input single-output (SISO) testbeds. Using a self-adaptive method, we assess a threshold close to the optimal, whereas the BER results are close to the minimum achievable. Furthermore, we show that for real existing molecular communication systems, an optimum can also be determined with respect to the BER. The BER can thus be reduced by up to 90 %.**

***Index Terms*—molecular communication (MC), bit error rate (BER), on-off keying (OOK), testbed, adaptive optimization**

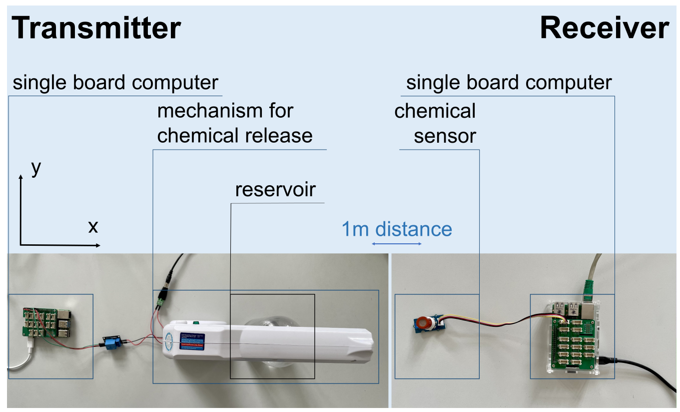

Fig. 1. The molecular SISO communication system. The system is not subject to any limitation and can be expanded at any time.

I. Introduction

Research in the nanotechnology field is becoming increasingly relevant due to the potential applications resulting from theoretical studies and experiments. Nanosensors are envisioned to advance precision medicine applications in the surveillance of physiological parameters of chronic patients, anytime, anywhere [1]. Besides, in industrial environments, nanosensors may survey the interior of pipes and defect damages and corrosion, extending the lifetime of industrial machines [2], [3]. Due to the tiny dimension of nanosensors and their limited resources, their actuator, and detection capabilities are primarily achieved cooperatively [4]. Nanosensors operating as nanonetworks may coordinate their resources to detect and actuate as a system, more effectively than individually. To achieve this, there is the need to effectively communicate between nanosensors through natural means using molecular communications (MCs) systems.

Supporting the nanocommunication infrastructure, single-input single-output (SISO) and multiple-input multiple-output (MIMO) MC-based systems have been widely studied in simulations, also including experimental designs [5]. Specifically, the use of MIMO in MC, although more complex, allows higher data rates (around 1.7) and a lower bit error rate (BER) (around 2.2 less), a rate difficult to achieve in SISO [6]. The spatial resources introduced by MIMO, in the connection of multiple emitters and receivers, allow for extending the bit rate or communication robustness as long as several channels are simultaneously used.

The implementation of SISO and MIMO systems are reported with macroscopic testbeds using liquid or air-based communication mediums [7]. Using inexpensive sprayers and sensors, realistic results are obtained when accounting for imperfections on the emitter and receiver sides. On the one hand, these testbeds illustrate the suitability to implement MIMO MC-based systems when recovering the emitted text message [8]. On the second hand, the communication performance is also evaluated through the resulting BER [9], the symbol error rate (SER) [10], and delay [11]. Besides, studies also outlines the impact of inter-symbol inteference (ISI) [11], [12], non-linearities of the channel [13], receptor susceptibility [14], and received signal level [15].

However, the above studies only conduct experiments for specific settings at the receiver. Little insights are provided on the optimal detector performance. When implementing the threshold detector, it is critical to set the proper threshold value, minimizing the perceived BER. Otherwise, the communication performance might result in heavily degraded.

Filling this gap, in this work we provide more insights into the optimal detection of incoming symbols as a resulting study from experiments. Specifically, using a SISO-MC testbed, as depicted in Fig. 1 (cf. Section II), we research on the optimal threshold to minimize the BER (cf. Section III). In this direction, we propose a low-complex adaptive algorithm for the self-optimization of SISO MC systems, as discussed in Section IV. The resulting method exhibits a close solution to the minimum BER and avoids the complexities of channel impulse response (CIR) estimation in real testbeds, where turbulences and non-linearities take place.

II. Testbed for Experiments

The testbed we conceive, as depicted in Fig. 2, is a macro-scale version of a molecular communication system according to the models in [12], [16]. The transmitter and the receiver are each equipped with a sprayer and a sensor – as a SISO testbed. The system is inexpensive and can be reprogrammed and modified as needed for research purposes. All used devices and sensors are commercial-off-the-shelf ones.

A. Hardware Layout

Fig. 1 shows the used hardware components of the testbed. The communication system consists of a molecular transmitter and receiver. The channel for propagation in between is one meter of free space. The propagation of the molecules is assisted by a standard fan. The active transport medium (air) consequently induces a higher mean number of received molecules [17]. The transmitter consists of *(i)* a single board computer (Raspberry Pi), used to execute coded algorithms on the transmitter side to encode and modulate the signal to be transmitted; *(ii)* a reservoir for chemicals as an alcoholic dissolution as diluted ethanol. The dissolution has a mass ratio of one part ethanol (H_3CCH_2OH) and three parts distilled water ($m_{H_3CCH_2OH}/m_{H_2O} = 1/3$); finally, *(iii)* a sprayer as a mechanism for chemical release of the molecules comprised of a mechanically controlled pump connected to a relay module. The relay module also allows controlling the amount of released molecules. The used commercial-off-the-shelf sprayer is the ninth generation of the wireless charging nano blue light atomizer (Inoxi Air Atomizer) [18]. A total of 1.50 g of 25 mass percent alcoholic solution is emitted per time interval of two seconds. This corresponds to a total of $N = 4.90 \times 10^{23}$ released molecules evaluated as

$$N = \frac{m}{M} \times N_A = \frac{1.50\text{g} \times 0.25}{46.07\frac{\text{g}}{\text{mol}}} \times 6.02 \times 10^{23} \frac{1}{\text{mol}}, \quad (1)$$

$$= 4.90 \times 10^{23} \quad (2)$$

where m, M, and N_A denote the mass of the released liquid per spray buff, the molar mass of ethanol [19], and the Avogadro constant.

The hardware of the receiver consists of *(i)* a chemical sensor for molecule detection as the MQ-3 Gas Sensor [20], and *(ii)* a single board computer (Raspberry Pi) forwarding the electrical signal from the chemical sensor, demodulating and decoding the received signal. The transmitter and also the receiver are connected wired to a local area network, so that the direct integration of molecular communication into conventional communication networks is possible. A computer, also located in the network, serves as the graphical user interface for the transmitter and receiver. Remote control of the single board computers is possible via secure shell.

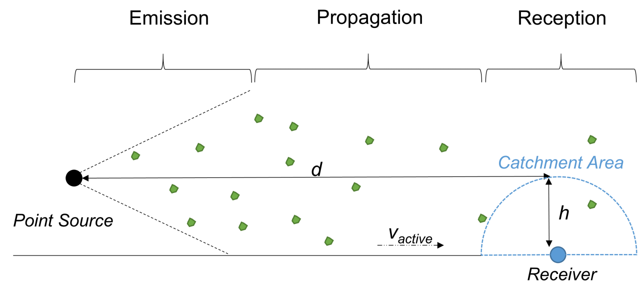

Fig. 2. System model of the testbed - side view. d, h, and v_{active} denote the distance between the transmitter and the receiver, the height of the transmission and the velocity of the fluid air (active medium).

TABLE I
Range of parameters used in the testbed.

Parameter	Variable	Value
Distance	d	1 m
Height of transmission	h	15 cm
Bit duration	T_b	2 sec
Threshold	τ	{0∼1000} mg/L
Bit sequence length		10
Mass of liquid for sending bit-1	m_1	1.50 g
Mass of liquid for sending bit-0	m_0	0 g
Flow speed	v	3.5 m/s
Diffusion coefficient	D	0.84×10^{-9} m^2/s

Fig. 2 illustrates main spatial parameters as a side view, where the parameter values are summarized in Table I. The transmission channel is free space diffusion in the medium air with flow supported by an air stream as BASETech Stand Fan FD-40A [21].

B. System Operation

The used modulation technique is the on-off keying (OOK). In this process, a constant number of molecules ($N = 4.90 \times 10^{23}$ cf. Eq. (1)) is emitted for the ones (cf. Fig. 3), and no molecules are released for the zeros in the digital sequence. During their transmission, the bit duration equals to $T_b = 2\,\text{sec}$.

In the coded algorithm on the transmitter side, the random bit sequences for the transmission are defined, where each sequence consists of $10\,\text{bit}$. The length is based on the international telegraph alphabet two (ITA2), which uses a sequence length of $5\,\text{bit}$ per character. Furthermore, on the transmitter side the bits are packed in frames consisting of three parts (as depicted in Fig. 4): a two bit start and synchronization sequence, a ten bit message sequence, and a five bit end sequence. The resulting emitted information is $58.8\,\%$ of the total of bits per packet. Transmissions always starts with the bit combination of '10' (start sequence), followed by the message sequence, and the end sequence, which concludes the packet transmission.

On the receiver side, the concentration of alcohol molecules is recorded as a voltage reading from the sensor. The demodulator compares the resulting voltage sequence to a threshold

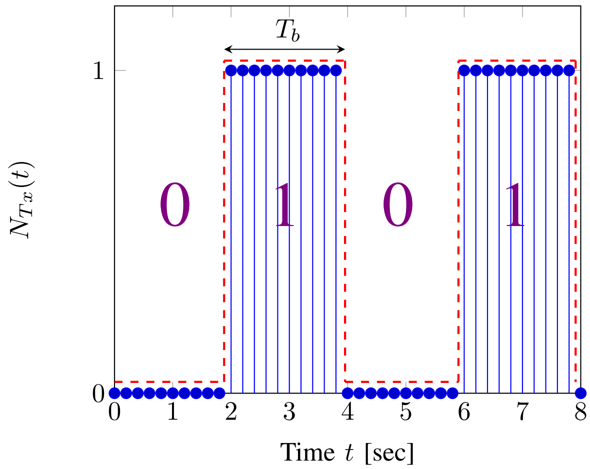

Fig. 3. Binary Channel Shift Keying (square waveform), following [22]. In BCSK, a variant of OOK, zeros are transmitted by no molecules and ones by a constant transfer of molecules over the entire time interval of the bit. N_{Tx}(t) denotes the number of released molecules, depending on the time. T_b describes the pulse duration of two seconds.

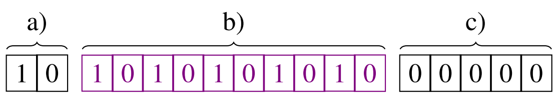

Fig. 4. Transmission scheme. a), b) and c) denote the two bit start sequence, the random ten bit message sequence, and the five bit end sequence.

to recover the sequence of bits. The threshold to decode incoming bits is conceived to be dynamically adjusted so that the decoding can be ensured in the following.

C. Synchronization

To recover the 5 bit per packet, two different algorithms are needed to detect the beginning and the end of the frame (cf. Fig. 4). Algorithm 1 and Algorithm 2 provide the algorithms on the receiver side for the two bit start/synchronization sequence, the message algorithm and the abort criterion.

Algorithm 1 Starting and synchronization algorithm for two bit sequence

while transmission **do**
  if measured value is greater than threshold **then**
    code ← *code*+ '1'
  else if measured value is smaller than threshold **then**
    code ← *code*+ '0'
  end if
  length ← *length of code*
  if length of the code is greater than two **then**
    if penultimate digit is a 1 and last digit is a 0 **then**
      Break for two seconds ▷ Time intervall BCSK
      Go to Algorithm 2
    end if
  end if
end while

The two algorithms each compare the measured value with a limit value and decode a higher concentration into a one and a lower concentration into a zero. The difference between the two algorithms clearly shows that a dynamic threshold is used in the start algorithm. That is, after each time step, the new threshold takes the value of the current measured value. Consequently, even a constant concentration of molecules leads to a bit flip from one to zero. In contrast, the threshold in the message algorithm is static, i.e., it does not change.

Algorithm 2 Message algorithm for ten bit sequence and abort criterion

Require: $threshold \geq 0$
while transmission **do**
  if measured value is greater than threshold **then**
    code ← *code*+ '1'
  else if measured value is smaller than threshold **then**
    code ← *code*+ '0'
  end if
  length ← *length of code*
  if length of the code is greater than four **and** length is multiple of five **then**
    if last five digits are 0 **then**
      Decode into the received bit sequence
      Break
    end if
  end if
end while

Then, the resulting sequence is sampled to detect the ones and the zeros, where the sampling time instants are checked by a synchronization mechanism. Thereby, after detecting the beginning and the end of the frame, the measurement will take place every two seconds in between as $T_b = 2\,\text{sec}$. A clock signal is provided every two seconds after the preamble is detected. As a result, the BER is to be measured. Therefor, the received bit sequences are compared with the transmitted bit sequences and are set in relation. Subsequently, the number of bit flips can be statistically determined, given the BER.

D. Health and Safety

Performing the experiments, low volumes of alcohol were diffused in open air. There are no chemical risks for a replica. The alcohol is safe for humans and is only used in diluted dissolution. The implementation was carried out behind a transparent shielded screen, so that unwanted damage due to the increased exposure to alcohol and humidity can be avoided.

III. BER Measurements Setup with the SISO Testbed

The SISO testbed we conceived, as described in Section II, let us evaluate the communication performance as the BER and its optimal operation as well. The perceived BER is highly dependent on the receiver threshold, which correctly determined allows the detection of the ones and the zeros from the incoming packets with the fewest possible errors. In this section, we provide experimental results on the dependency of the BER with the threshold, which eventually let to corroborate reported theoretical expressions as well [23].

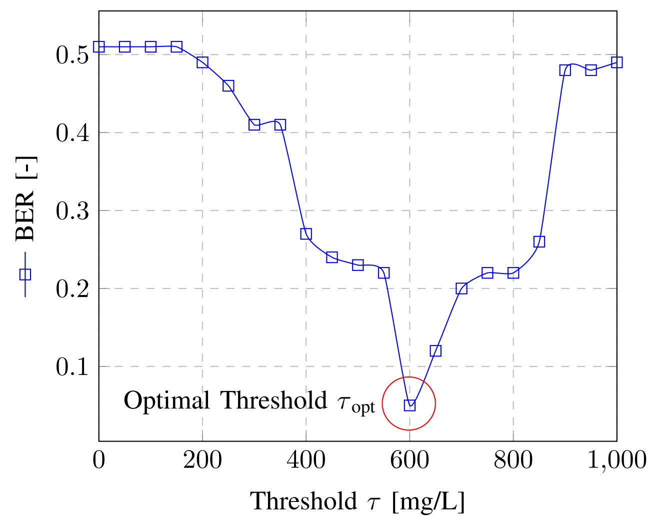

Fig. 5. Primary BER vs. threshold τ. The figure is based on the experimental setup, f.e. real data. The optimal threshold τ_{opt} denotes the threshold for the lowest BER of the communication system using OOK.

A. BER Measurements

For the evaluation of the threshold τ, the concentration of alcohol molecules measured by the sensor is used. The range of values extends as 0–1000 mg/L, whereby the limits of the interval are not reached at any time ($0 < \tau < 1000$). As shown in Section II, random ten-digit bit sequences with a respective start and end sequence are transmitted so that a synchronization of the transmitter and receiver can be achieved. To perform the measurements, the number of transmitted bits was fixed. For evaluation and statistical analysis, 300 bit were transmitted for every certain threshold.

Fig. 5 shows the dependence of the BER on the threshold τ. The minimum of the BER is observed for a threshold of 600 mg/L. For the range left of the optimum, the BER increases to the maximum of 0.5 or 50 %. With the approach towards the threshold to zero, the threshold is exceeded for each bit – consequently a one is always decoded; thereby resulting in half of the total of bits with errors. To the right side of the optimum threshold, the behavior is analogous. With increasing limit value, always only zeros are decoded, since the target value cannot be reached.

In general, it can be concluded that on the left side the BER for a transmitted zero decreases and on the right side the BER for a transmitted one increases – analogous to [24] as a concave function. The unevenness of the graph results in the actual measured values and the experimental setup. Turbulence in the air flow leads to inaccuracies in the transfer, and inhomogeneous mixing leads to fluctuations in the concentration of alcohol molecules. In addition, only 21 threshold intervals were examined in the testbed, in contrast to a significantly higher number in the simulations.

B. Comparison to Reported Simulation

Compared to previous simulations, a similar picture emerges. In [24] a minimum of the BER already shows up at a threshold of 250 (with logarithmic axis division of the ordinate axis). The two curves are concave, with only one minimum, depending on the different parameters shown in Table I.

It becomes clear that the simulated results substantiate the experimental testbed setup. The differences in the optimal threshold between simulation and experiment can be attributed to various parameters of the system. Among others, the concentration of the liquid/number of emitted molecules, the distance between the emitter and the receiver, the influence of the active transport medium, the sensitivity of the sensors or the length of the selected time interval should be mentioned.

The higher the concentration of the alcohol solution or the number of molecules, the greater the impact of ISI at the receiver. Consequently, the threshold is very easily exceeded – the optimum shifts to the right. The situation is analogous for a lower number of diffusing molecules – the limit value shifts to the left. Another influencing parameter is the distance between transmitter and receiver. The greater the distance, the fewer molecules diffuse to the receiver in the time interval. The minimum of the BER shifts to the left. A third decisive parameter is the channel; diffusion with drift will produce an increased number of molecules in the effective range of the receiver. The concentration increases and the optimum shifts to the right.

IV. Self-Adaptive Algorithm

This section proposes an adaptive algorithm for self-optimizing a MC system based on an adaptive-based mechanism. We plan to evaluate the cross-correlation between emitted patterns and decoded ones as a way to find the optimum threshold. Intuitively, whenever the threshold is far from the optimum, the decoded sequence will not be similar to the emitted pattern due to errors; thus, the cross-correlation will display a low value. On the contrary, whenever the threshold is in the vicinity of the optimum, the resulting cross-correlation will be higher.

To illustrate, Fig. 6 depicts the resulting cross-correlation using an alternate pattern of 1's and 0's versus the received threshold. The curves depict a maximum where the sequence is decoded correctly; thus, for the smaller BER. Considering this is a concave function with a global maximum, we can implement a gradient-based algorithm to get the threshold close to the optimum [25]. That is, by computing the gradient vector with two measurements, we can distinguish the proper direction to update the value of τ. Whenever the gradient slope is positive (left vector in Fig. 6), we increase the value of τ; otherwise, we decrease it (right vector in Fig. 6).

The algorithm was developed and implemented for the SISO MC system presented in Section II, but can be scaled to other systems. It is used to update the threshold value for the decoder, as depicted in the schematic from Fig. 7. The cross correlation is implemented according to

$$R_{T,R} = \sum t_x[n] \times r_x[n], \tag{3}$$

where r_x, t_x, τ, τ_{opt} and $R_{T,R}(\tau)$ denote the received sequence, the transmitted sequence, the adapted threshold,

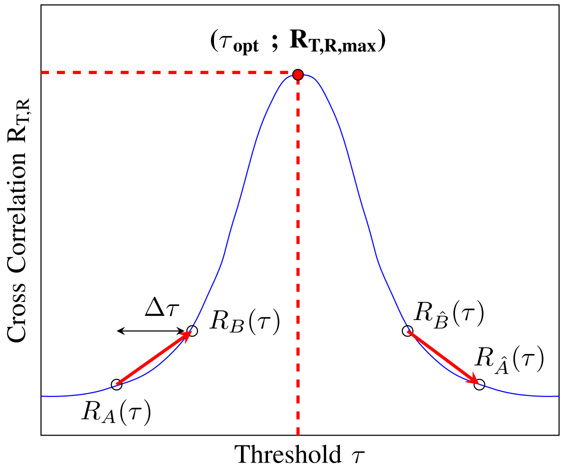

Fig. 6. Dependence of the optimal threshold τ_{opt} on the cross-correlation $R_{T,R}$. For the localization of the right or left side of the extremes, the sampling points A and B or Ã and B̃ with a difference interval of $\Delta\tau$ are used.

the optimal threshold and the cross correlation between the transmitted and received sequence. Besides, to calculate the cross-correlation, the value −1 is used for a transferring zero, so that the results can be obtained both to the left and to the right of the optimum.

The algorithm for self-optimization of the molecular communication system starts with the synchronization algorithm, following Algorithm 1. The sequence can be of any even length, due to the algorithm with boundary cross correlation of 0, and alternates between 0 and 1 or between -1 and 1 for the cross-correlation, i.e., for a sequence length of 10 bits [0,1,0,1,0,1,0,1,0,1]. The algorithm update the threshold value per iteration according to $\tau_{\text{new}} = \tau_{\text{old}} + \Delta\tau_{\text{new}}$, where the steps are updated according to $\Delta\tau_{\text{new}} = \Delta\tau \times r_f$, and r_f is a reduction factor in the set $[-1, 1]$. The algorithm operates by computing two times the cross-correlation as Eq. (3) for two values of τ. Whenever $R_A(\tau) \leq R_B(\tau)$ then r_f is set to 1, otherwise to −1. The corresponding reduction amount can be freely selected, although we report results when $r_f = 1 - 0.1 = 0.9$ (reduction by 10 %).

The authors have successfully implemented the algorithm for the testbed presented in Section II. Fig. 8 shows the real results of the implementation. The threshold τ, starting from the estimated threshold $\tau_{est} = 500$, approaches the optimal threshold τ_{opt} in $\Delta\tau = 50$ steps. When the optimal threshold is reached, the algorithm terminates because the optimum has been achieved. Due to the step size selected with $\Delta\tau = 50$, no

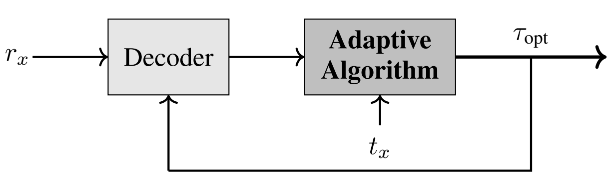

Fig. 7. Basic operation scheme for the self-optimization algorithm of a MC system using OOK on the receiver side.

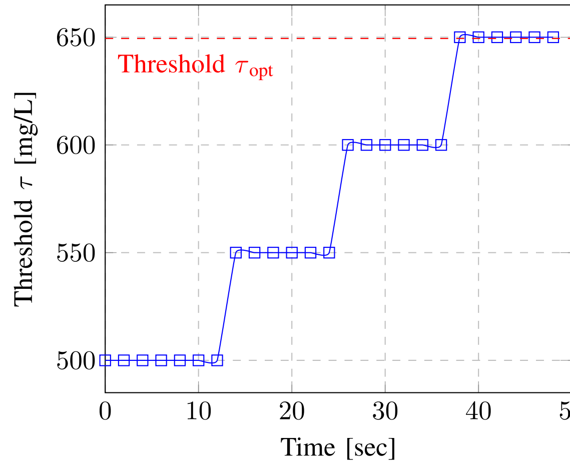

Fig. 8. Approximation of the optimal limit based on the algorithm. The following estimates and parameters were chosen for the evaluation of the algorithm: $\tau_{est} = 500$, $\Delta\tau = 50$, and r_f=0.9.

oscillation around the optimal threshold τ_{opt} can be detected.

V. Conclusion

In this paper, we presented a low-complex adaptive algorithm to determine the threshold in SISO-MC systems minimizing the BER. Through measurements, the algorithm evidences good performance running in real testbeds, which exhibit their robustness in real scenarios. Furthermore, we show that for real existing molecular communication systems, an optimum can also be determined with respect to the BER. Future research is in the direction of implementing a more efficient adaptive-based mechanism to provide much more accurate results for the threshold. We also aim to extend the testbed towards MIMO

Acknowledgments

This work was supported by the German Research Foundation (DFG) as part of Germany's Excellence Strategy—EXC 2050/1—Cluster of Excellence "Centre for Tactile Internet with Human-in-the-Loop" (CeTI) of TU Dresden under grant 390696704 and the 6G-life project supported by the Federal Ministry of Education and Research (BMBF) under grant 16KISK001K. The work was also supported by the project MAMOKO funded by the German Federal Ministry of Education and Research (BMBF) under grant 16KIS0917 and the project NaBoCom funded by the German Research Foundation (DFG) under grant DR 639/21-1.

References

[1] M. Peleg, Y. Shahar, and S. Quaglini, "MobiGuide," *Communications of the ACM*, vol. 65, no. 4, pp. 74–79, 4 2022.

[2] W. Haselmayr, A. Springer, G. Fischer, C. Alexiou, H. Boche, P. A. Hoeher, F. Dressler, and R. Schober, "Integration of Molecular Communications into Future Generation Wireless Networks," in *1st 6G Wireless Summit*. Levi, Finland: IEEE, 3 2019.

[3] Y. Lu, R. Ni, and Q. Zhu, "Wireless Communication in Nanonetworks: Current Status, Prospect and Challenges," *IEEE Transactions on Molecular, Biological and Multi-Scale Communications*, vol. 6, no. 2, pp. 71–80, 11 2020.

Algorithm 3 Self-Optimization Algorithm for OOK

Require: Synchronization (Algorithm 1)

$\tau \leftarrow$ *input (estimate value* τ_{est}*)*
$\Delta\tau \leftarrow$ *input*
$l \leftarrow$ *0*
$r \leftarrow$ *0*
$r_f \leftarrow$ *input*
while transmission **do**
  if measured value is greater than threshold τ **then**
    $code_A \leftarrow code_A +$ '1'
  else if measured value is smaller than threshold τ **then**
    $code_A \leftarrow code_A +$ '-1'
  end if
  $length_A \leftarrow$ *length of code*
  if length is equal to number of transmitted bits n **then**
    $R_A \leftarrow$ *cross correlation of* r_x *and* t_x
  end if
  $\tau_{new} \leftarrow \tau + \Delta\tau$
  if measured value is greater than threshold τ_{new} **then**
    $code_B \leftarrow code_B +$ '1'
  else if measured value is smaller than theshold τ_{new} **then**
    $code_B \leftarrow code_B +$ '-1'
  end if
  $length_B \leftarrow$ *length of code*
  if length is equal to number of transmitted bits n **then**
    $R_B \leftarrow$ *cross correlation* r_x *and* t_x
  end if
  if R_B is greater than R_A **then**
    $\tau_i \leftarrow \tau + \Delta\tau$ ▷ left side
  end if
  if R_A is greater than R_B **then**
    $\tau_i \leftarrow \tau - \Delta\tau$ ▷ right side
  end if
  if R_A is equal to R_B is equal to 0 **and** last character of the received code is equal to 1 **then**
    $\tau_i \leftarrow \tau - \Delta\tau$ ▷ boundary right
  else if R_A is equal to R_B is equal to 0 **and** last character of the received code is equal to -1 **then**
    $\tau_i \leftarrow \tau + \Delta\tau$ ▷ boundary left
  end if
  if l is equal to r is equal to 1 **then**
    $\Delta\tau \leftarrow \Delta\tau \times r_f$ ▷ optimum in between
  end if
  if R_A is equal to R_B is equal to n **then**
    $\tau_{opt} \leftarrow \tau$
    transmission end
  end if
end while

[4] F. Dressler and O. B. Akan, "Bio-inspired Networking: From Theory to Practice," *IEEE Communications Magazine*, vol. 48, no. 11, pp. 176–183, 11 2010.

[5] A. Al-Helali, B. Liang, and N. Nasser, "Novel Molecular Signaling Method and System for Molecular Communication in Human Body," *IEEE Access*, vol. 8, pp. 119 361–119 375, 1 2020.

[6] B. H. Koo, C. Lee, H. B. Yilmaz, N. Farsad, A. W. Eckford, and C. B. Chae, "Molecular mimo: From theory to prototype," *IEEE Journal on Selected Areas in Communications*, vol. 34, no. 3, pp. 600–614, 3 2016.

[7] S. Bhattacharjee, M. Damrath, F. Bronner, L. Stratmann, J. P. Drees, F. Dressler, and P. A. Hoeher, "A Testbed and Simulation Framework for Air-based Molecular Communication using Fluorescein," in *ACM NANOCOM*. ACM, 9 2020.

[8] C. Lee, B.-H. Koo, and C.-B. Chae, "Demo: In-Vessel Molecular MIMO Communications," in *IEEE WCNC, Workshops*. Seoul, South Korea: IEEE, 4 2020.

[9] L. Khaloopour, S. V. Rouzegar, A. Azizi, A. Hosseinian, M. Farahnak-Ghazani, N. Bagheri, M. Mirmohseni, H. Arjmandi, R. Mosayebi, and M. Nasiri-Kenari, "An Experimental Platform for Macro-Scale Fluidic Medium Molecular Communication," *IEEE Transactions on Molecular, Biological and Multi-Scale Communications*, vol. 5, no. 3, pp. 163–175, 12 2019.

[10] Y. Huang, M. Wen, L.-L. Yang, C.-B. Chae, X. Chen, and Y. Tang, "Space Shift Keying for Molecular Communication: Theory and Experiment," in *IEEE GLOBECOM*. Waikoloa, HI: IEEE, 12 2019.

[11] S. Qiu, W. Guo, S. Wang, N. Farsad, and A. Eckford, "A molecular communication link for monitoring in confined environments," in *IEEE ICC, Workshops*. Sydney, Australia: IEEE, 6 2014.

[12] N. Farsad, W. Guo, and A. W. Eckford, "Tabletop Molecular Communication: Text Messages through Chemical Signals," *PLOS ONE*, vol. 8, no. 12, pp. 1–13, 12 2013.

[13] D. T. Mcguiness, S. Giannoukos, A. Marshall, and S. Taylor, "Modulation Analysis in Macro-Molecular Communications," *IEEE Access*, vol. 7, pp. 11 049–11 065, 1 2019.

[14] H. Unterweger, J. Kirchner, W. Wicke, A. Ahmadzadeh, D. Ahmed, V. Jamali, C. Alexiou, G. Fischer, and R. Schober, "Experimental Molecular Communication Testbed Based on Magnetic Nanoparticles in Duct Flow," in *IEEE SPAWC*, Kalamata, Greece, 6 2018.

[15] D. T. McGuiness, S. Giannoukos, A. Marshall, and S. Taylor, "Parameter Analysis in Macro-Scale Molecular Communications Using Advection-Diffusion," *IEEE Access*, vol. 6, pp. 46 706–46 717, 5 2018.

[16] N.-R. Kim, N. Farsad, C.-B. Chae, and A. Eckford, "A realistic channel model for molecular communication with imperfect receivers," 06 2014.

[17] H. ShahMohammadian, G. G. Messier, and S. Magierowski, "Nano-machine molecular communication over a moving propagation medium," *Nano Communication Networks*, vol. 4, pp. 142–153, 2013.

[18] *Data sheet Inoxi Atomizer*, Sips Hygiene Evolution, https://www.reinigungsberater.de/dokumente/vernebler_inoxi_air_atomizer_elektrischer_zerstaeuber_weiss,p-8510516,dl-produktblatt.pdf – Accessed: 2022/05/30.

[19] PubChem, "Ethanol," https://pubchem.ncbi.nlm.nih.gov/compound/702 – Accessed: 2022/30/05. [Online]. Available: https://pubchem.ncbi.nlm.nih.gov/compound/702

[20] *Technical Data MQ-3 Gas Sensor*, Hanwei Electronics Co., LTD, https://files.seeedstudio.com/wiki/Grove-Gas_Sensor-MQ3/res/MQ-3.pdf – Accessed: 2022/06/01.

[21] *Stand fan 50 W, Item no. 1379641*, BASETech, https://www.manualslib.de/manual/125129/Basetech-1379641.html – Accessed: 2022/06/01.

[22] H. B. Yilmaz, N.-R. Kim, and C.-B. Chae, "Effect of ISI mitigation on modulation techniques in communication via diffusion," *ArXiv*, 2014.

[23] L. Brand, S. Lotter, V. Jamali, and R. Schober, "Area Rate Efficiency in Molecular Communications," in *ACM NANOCOM*. Catania, Italy: ACM, 9 2021.

[24] P. He, Y. Mao, Q. Liu, and K. Yang, "Improving reliability performance of diffusion-based molecular communication with adaptive threshold variation algorithm," *International Journal of Communication Systems*, vol. 29, no. 18, pp. 2669–2680, 2016.

[25] S. Haykin, *Adaptive filter theory*, 5th ed. Prentice Hall, 2013.